Supplementary Table 1

| Embryo number | Normal ventriculo-arterial connections | VSD | Aortic valve | Pulmonary valve | Ectopic coronary arteries | SMC disorganisation | Elastin disorganisation |
|---|---|---|---|---|---|---|---|
| 1 | N | N | DT | DT | N | A | A |
| 2 | D | V | DB | DB | E | A | A |
| 3 | N | N | DB | DT | E | A | N |
| 4 | N | N | DB | T | E | A | A |
| 5 | N | N | DT | T | E | A | A |
| 6 | N | N | T | T | E | A | N |
| 7 | N | N | DT | DT | N | A | N |
| 8 | N | N | DB | DT | N | A | N |
| 9 | N | N | DB | DT | E | A | N |
| 10 | N | N | DT | DT | N | A | N |
| 11 | N | N | DB | DT | E | A | A |
| 12 | N | N | DT | DT | E | A | N |
| 13 | N | N | DT | DT | N | N | N |
| 14 | N | N | DB | DT | E | A | N |
| 15 | N | N | DQ | DT | E | A | N |
| 16 | D | V | T | T | E | A | N |
| 17 | N | N | T | DT | E | A | N |
| 18 | D | V | DB | DT | E | A | N |
| 19 | D | V | DT | DT | E | A | Y |
| 20 | N | N | DQ | DT | E | A | N |
| 21 | D | V | DB | DT | E | A | A |
| 22 | D | V | DB | DT | E | - | - |
| 23 | D | V | DT | DT | E | - | - |
| 24 | D | V | DT | DT | E | - | - |
| 25 | D | V | DB | DB | E | - | - |
| 26 | D | V | DB | DB | N | - | - |
| 27 | D | V | DT | DT | N | - | - |
| 28 | D | V | DB | DT | E | - | - |
| 29 | N | N | DQ | DQ | E | - | - |
| 30 | N | N | DT | T | E | - | - |
| 31 | N | N | T | DQ | E | - | - |

A = abnormal, B = bicuspid, D = double outlet right ventricle, DB = dysplastic bicuspid, DT = dysplastic tricuspid, E = ectopic, N = normal, Q = quadricuspid, V = ventricular septal defect, - = not scored

**Supplementary Table 1**: Anatomical scoring for each E14.5-E15.5 *RockDN;Wnt1-cre* embryo included in the analysis

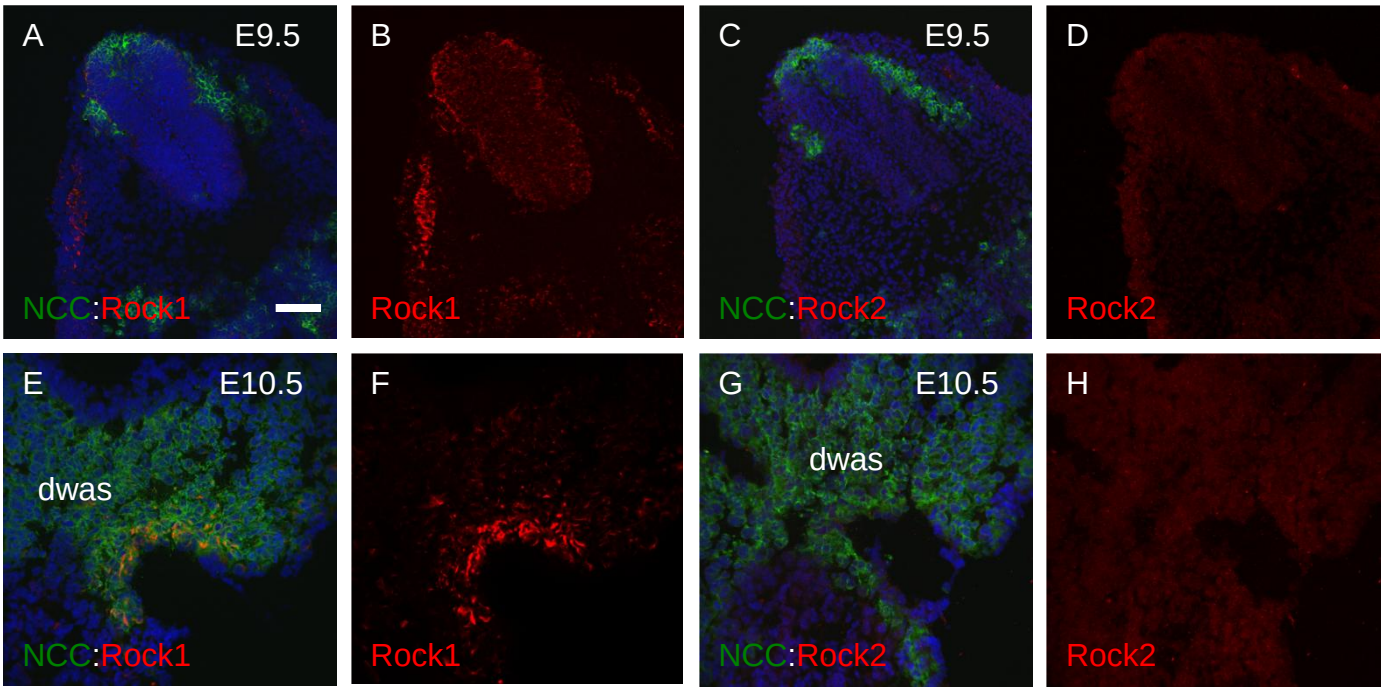


**Suppl Figure 1. Expression pattern of Rock1 and Rock2 in NCC.** Sections are from E9.5 and E10.5 *Wnt1-cre;ROSAeYFP* embryos; the sections are stained with an antibody that recognises eYFP (green) and Rock1 or Rock2 (red). Rock1 does not appear to be expressed in the dorsal neural tube or the migrating NCC (**A,B**), but is expressed in NCC within the dorsal wall of the aortic sac (**E,F**). Rock2 is found at only low levels, or is undetectable, in the dorsal neural tube (**C,D**) in the aortic sac (**G,H**). dwas = dorsal wall of the aortic sac. Scale bar A-D = 200µm, E-H = 50µm.

Supplementary Figure 2

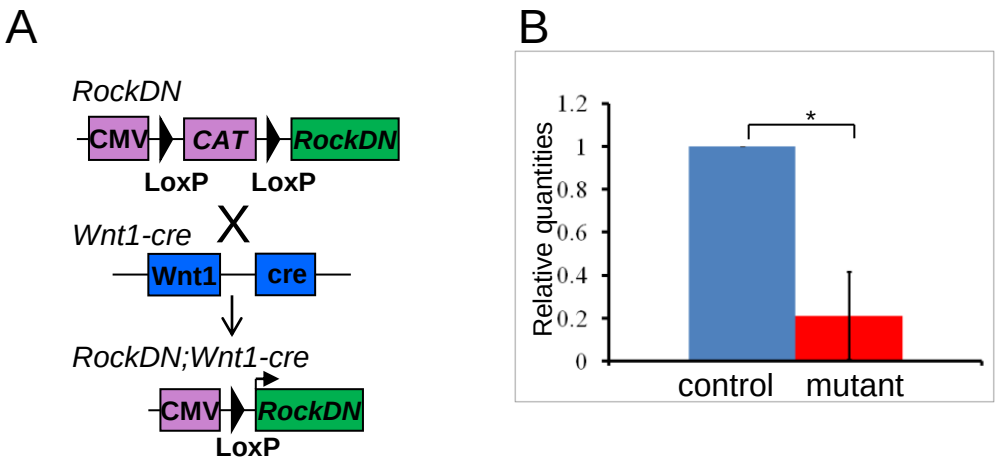


**Suppl Figure 2. Breeding strategy of the *RockDN* mice. A**) The *RockDN* mice were mated with *Wnt1-cre* mice which removed the *CAT* box, allowing expression of the Rock dominant negative protein. **B**) Removal of the *CAT* box was confirmed by qPCR using outflow tracts dissected from E11.5 control and mutant littermates. Using a one way Anova test, a statistically significant decrease ($P<0.05$ *) in the expression of the *CAT* box was observed in the mutant outflow tracts, compared to the control embryos.

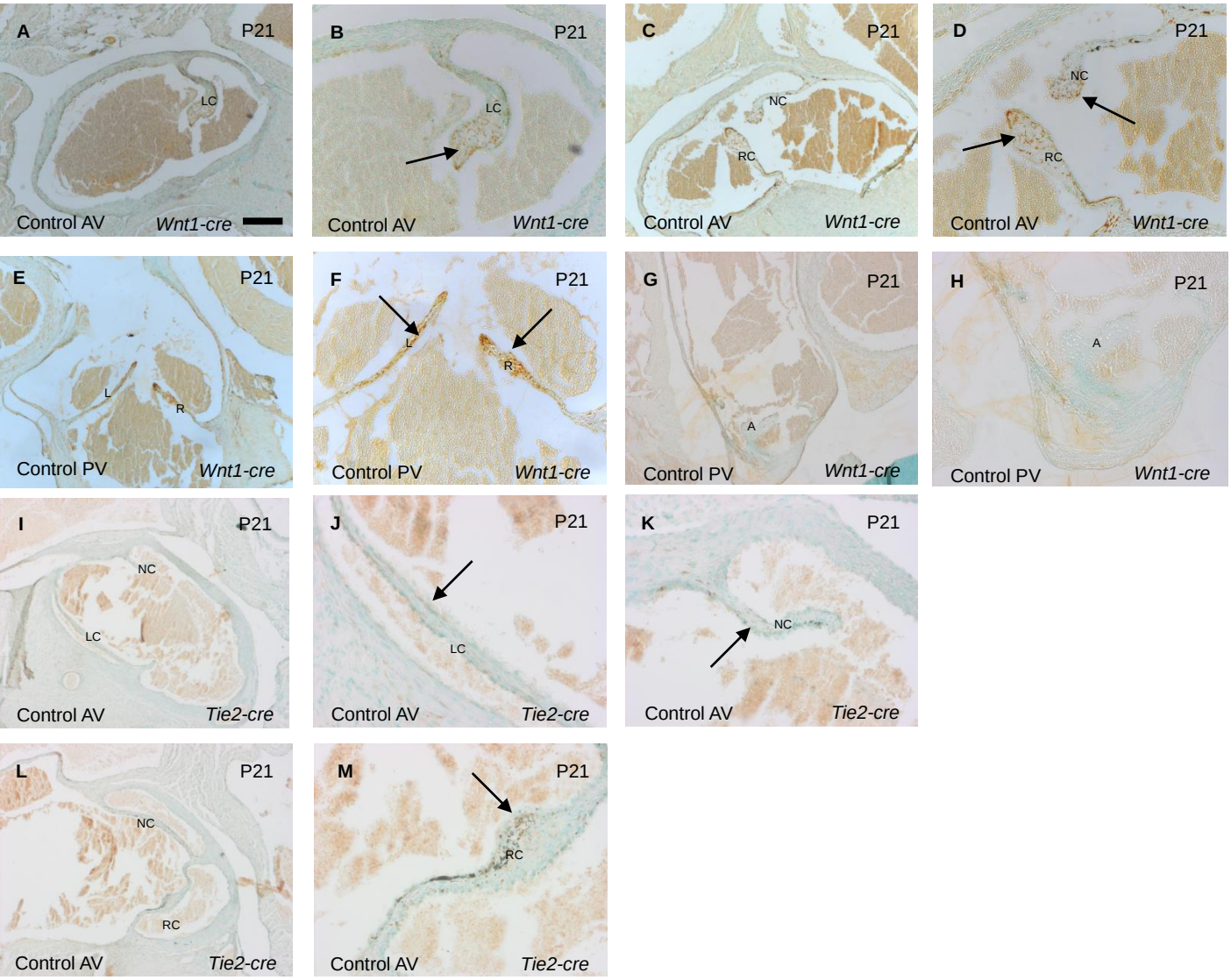


**Suppl Figure 3. NCC are found in arterial valve leaflets postnatally.** Transverse sections taken through a *Wnt1-cre;ROSAeYFP* heart at P21 (A-H) and a *Tie2-cre;ROSAeYFP* heart at P21 (I-M), were stained with an antibody that recognises eYFP. NCC are abundant in all the aortic valve leaflets (**A-D**) and in the left and right leaflets of the pulmonary valve (**E,F**), with very few found in the anterior leaflet (**G,H**). Endothelial cells are also found in the arterial valve leaflets (**I-M**).
A = anterior, AV = aortic valve, L = left, LC = left coronary, NC = non-coronary, PV = pulmonary valve, R = right, RC = right coronary. Scale bar A,C,E,G,I,L = 100µm, B,D,F,H,J,K,M = 50µm.

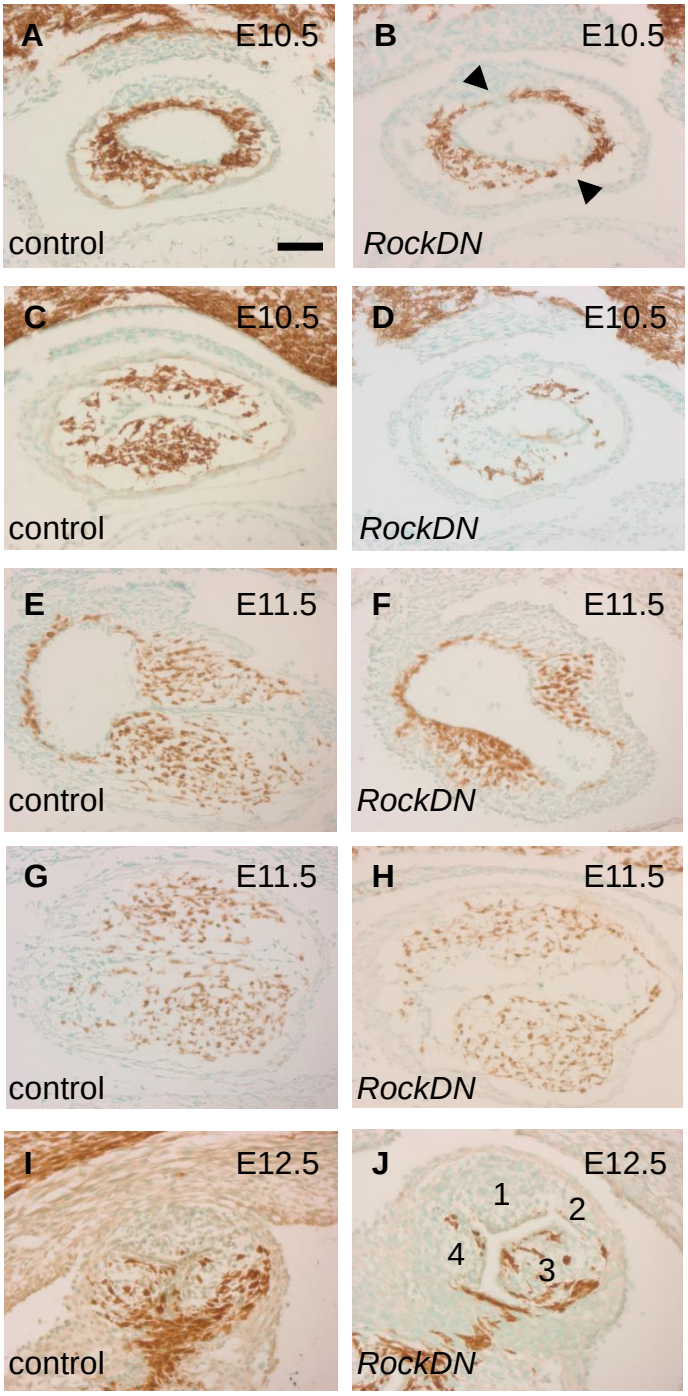


**Suppl Figure 4. Further examples of abnormal positioning of outflow tract cushions.** All the sections are coronal and the NCC are stained brown. **A-D**) At E10.5 the NCC in the distal outflow tract are arranged uniformly in the control (A) but there are gaps between NCC in the mutant (arrowheads in B). More proximally, the NCC are aggregating into two discrete cushions in the control (C); this process is delayed in the mutant (D). **E-H**) At E11.5 the distal (E) and mid region (G) outflow cushions are fused or fusing in the control. In contrast, the cushions are widely separated in the *RockDN* mutant and they are abnormally positioned and sized (F,H). **I,J**) The pulmonary valve leaflets are abnormally sized and positioned at E12.5 in the mutant, with four discrete leaflets apparent (J).
Scale bar A-J = 50µm.

Supplementary Figure 5

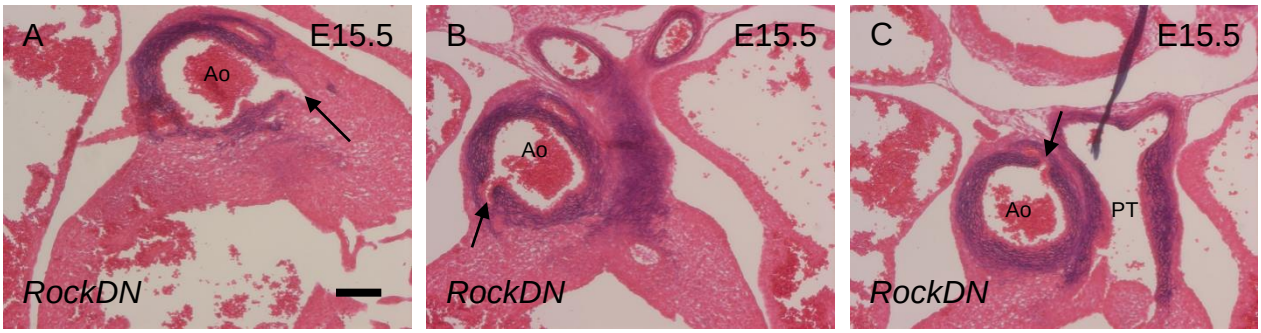


**Suppl Figure 5. Abnormal coronary arteries in a *RockDN;Wnt1-cre* mutant.** In one mutant at E15.5, three coronary arteries arose from the left (**A**), right (**B**) and non-coronary sinuses (**C**).
Ao = aorta, PT = pulmonary trunk. Scale bar A-C = 100µm.

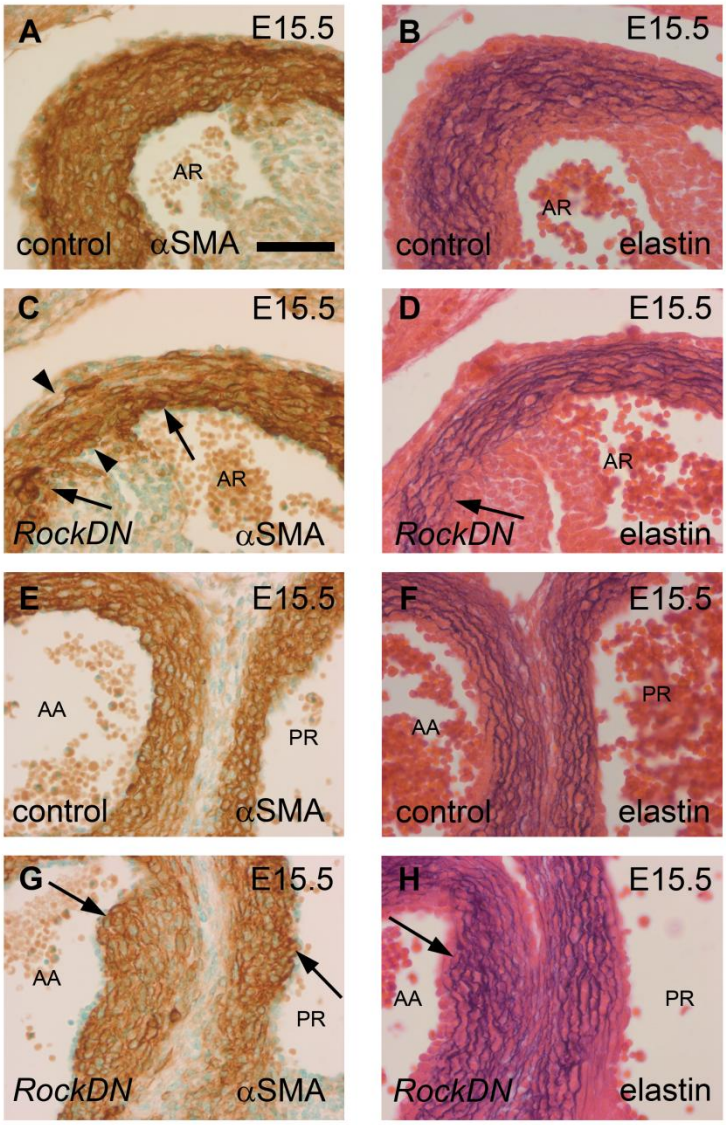


**Suppl Figure 6. Arterial wall abnormalities in *RockDN;Wnt1-cre* mutants at E15.5.** A,B,E,F are control embryos, C,D,G,H are *RockDN;Wnt1-cre* mutants. **A,C,E,G)** αSMA staining (brown) is disrupted in both the aortic (C) and pulmonary (G) roots and in the ascending aorta (G) in mutant embryos (arrows), suggesting that SMC are differentiating abnormally. Moreover, the arterial wall is thickened in the ascending aorta (G, arrow). **B,D,F,H)** Elastin (black) deposition is somewhat disorganised in mutant embryos, correlating with SMC disorganisation. AA = ascending aorta, AR = aortic root, PR = pulmonary root. Scale bar A-H = 50µm.

Supplementary Figure 7

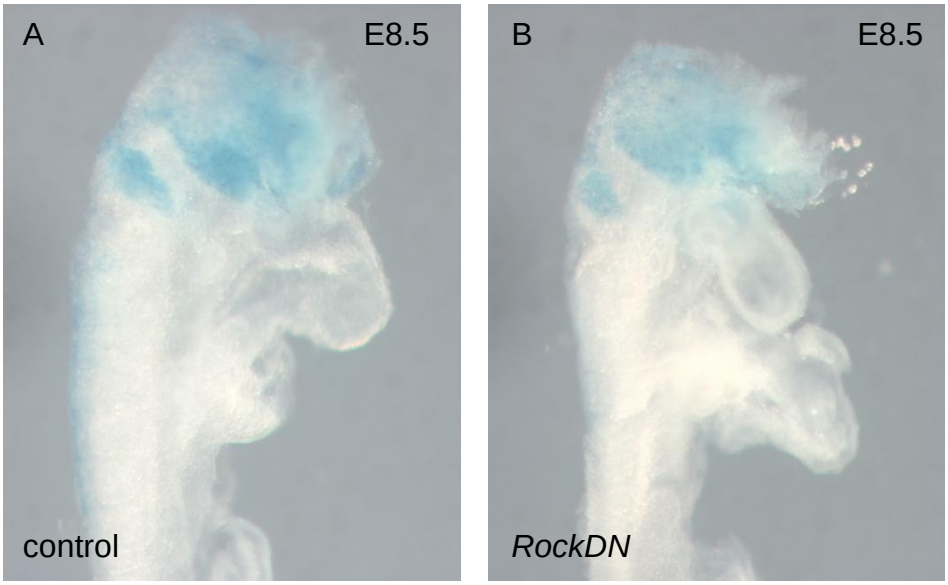


**Suppl Figure 7. Delamination and migration of NCC.** *RockDN;ROSA 26R* mice were crossed with *Wnt1-cre* mice and the embryos were LacZ stained to show the position of the NCC. At E8.5 (**A,B**) the delamination and early migration of the NCC was normal in the *RockDN;Wnt1-cre* mutant (B).

Supplementary Figure 8

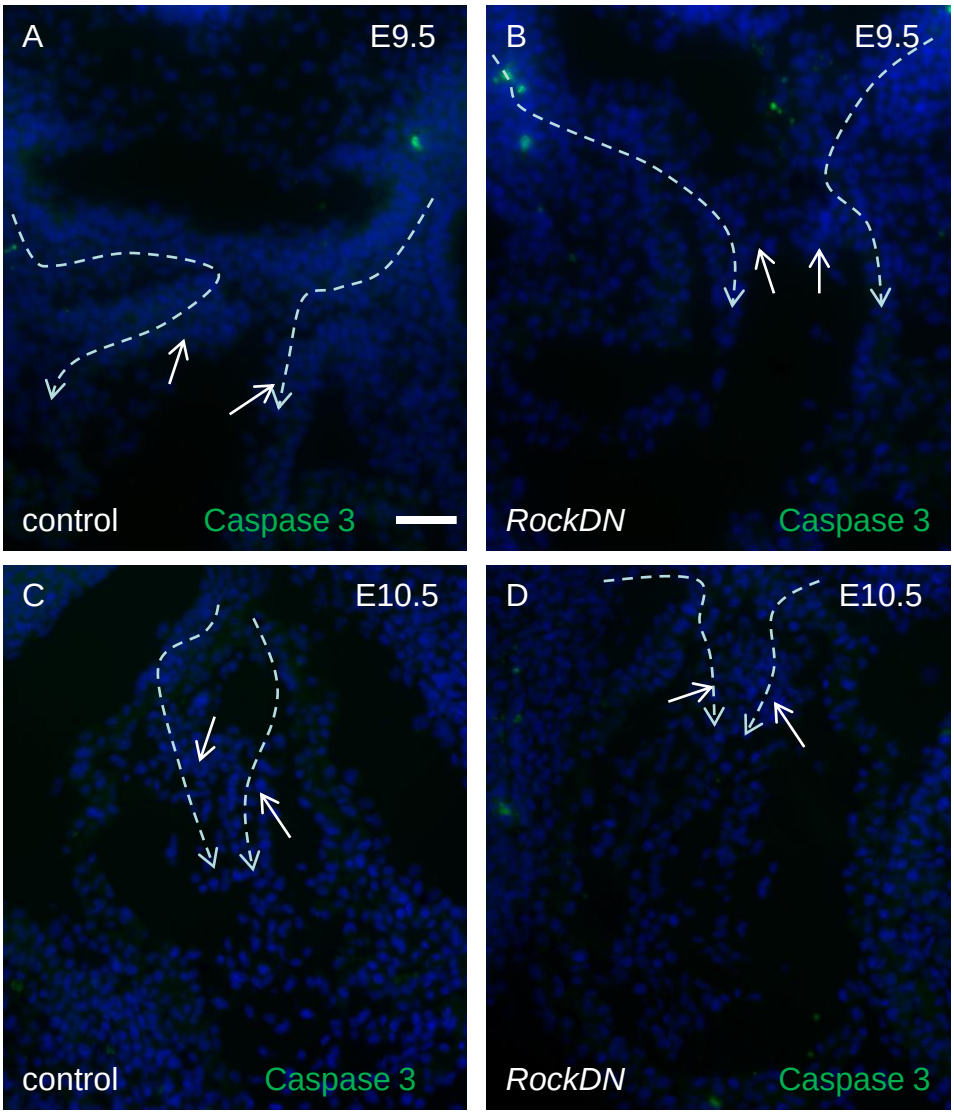


**Suppl Figure 8. Absence of cell death within the outflow tract.** Transverse sections through the outflow tract at E9.5 and E10.5 were stained for cleaved caspase 3 to identify any cells undergoing cell death. The white dashed line shows the direction of migration of the neural crest cells. There was no cell death within the cushions (arrows) in the controls or mutants at these stages.
Scale bar A-D = 100μm.

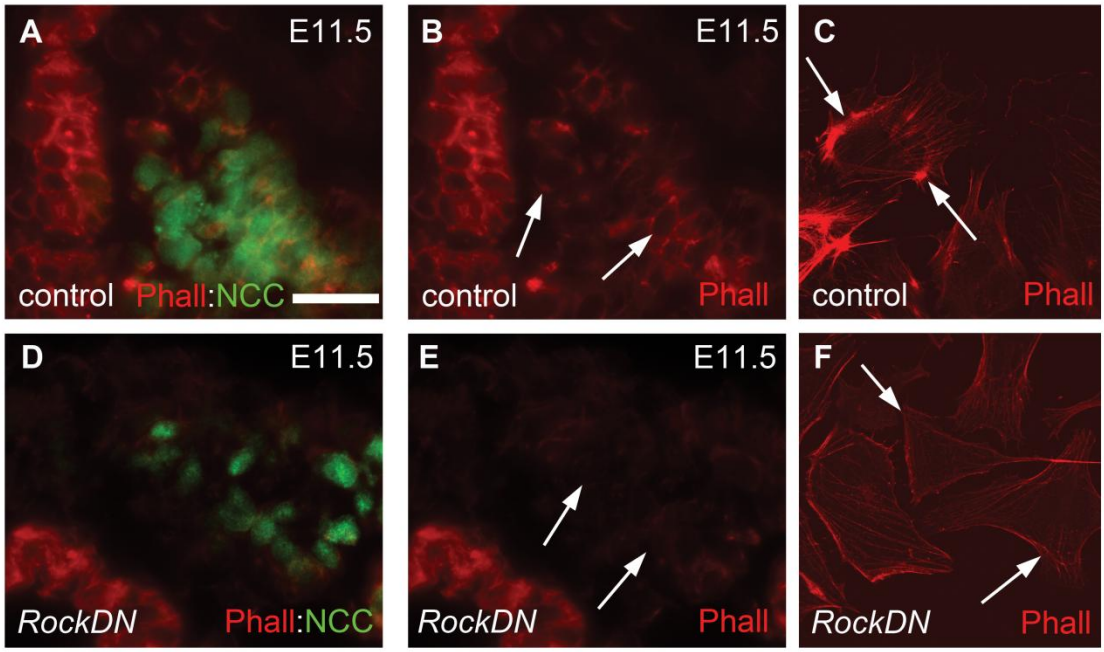


**Suppl Figure 9. Loss of actin cytoskeleton in outflow tract neural crest cells.** A,B,D,E are transverse sections and C,F are NCC from *in vitro* cultures. The actin cytoskeleton is stained using Phalloidin (red) and NCC are labelled using the GFP antibody (green). **A,B,D,E)** The NCC in E11.5 control embryos displayed cortical stress fibres, whereas in the *RockDN;Wnt1-cre* embryos these were missing or reduced (compare arrows in B and E). **C,F)** *In vitro*, NCC cultures isolated from control E9.5 embryos displayed actin stress fibres strongly at the rear and lateral sides of the cells (arrows in C). Filamentous actin staining is reduced in isolated NCC from *RockDN;Wnt1-cre* embryos (arrows in F). Phall = phalloidin. Scale bar A,B,D,E = 50µm, C,F = 20µm.

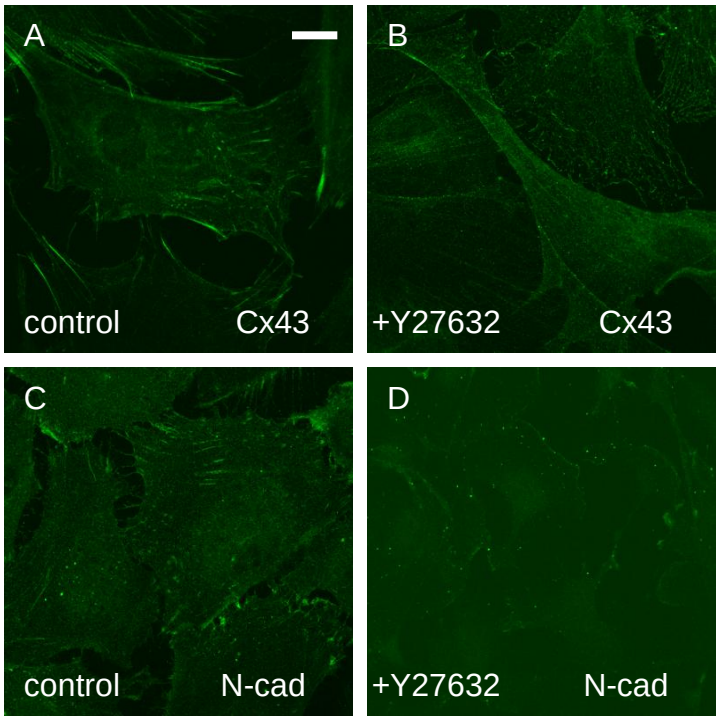


**Suppl Figure 10. *In vitro* analyses of Rock inhibition.** NCC from *in vitro* cultures. Cx43 (**A,B**) and N-cadherin (**C,D**) expression are both reduced at the cell membrane and cell-cell contacts in Rock inhibitor-treated cells. Cx43 = connexin 43, N-cad = N-cadherin.
Scale bar = 15µm.

Supplementary Figure 11

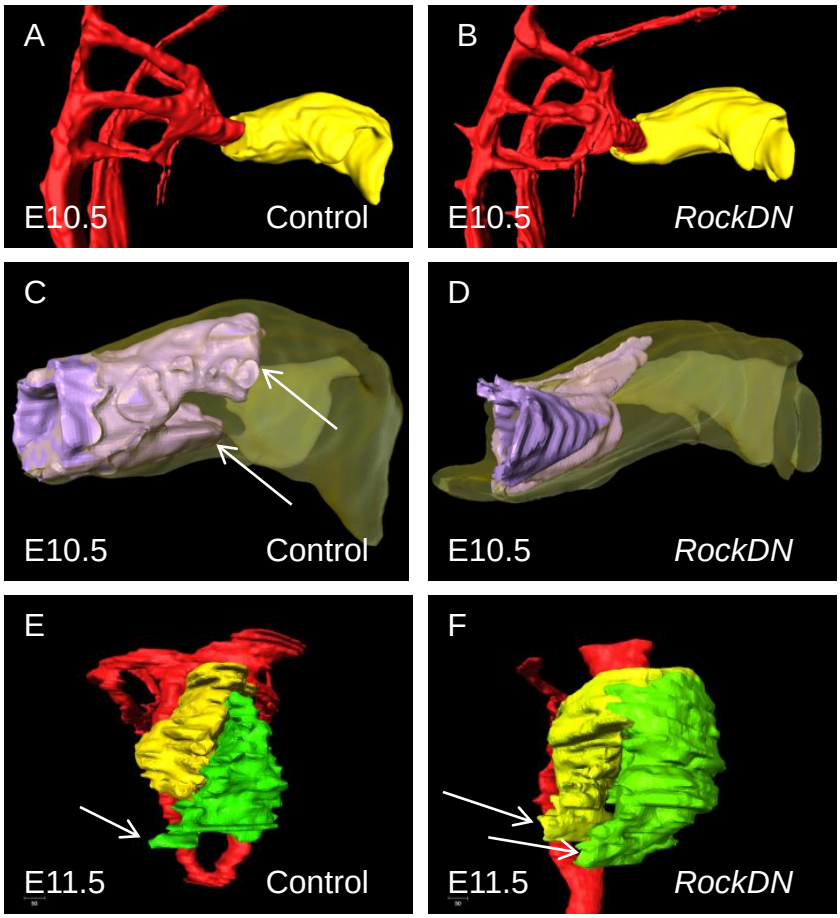


**Suppl Figure 11. 3D reconstructions of outflow tract cushions in *RockDN;Wnt1-cre* mutants.** The lumen of the pharyngeal arch arteries and descending aorta (red) are included for reference. **A,B)** The cardiac jelly was painted in control and *RockDN;Wnt1-cre* mutant embryos at E10.5. The basic form of these structures is very similar at this stage. **C,D)** Enlargement of the outflow tract with the cardiac jelly now painted in grey and NCC painted in purple. Although the NCC are circumferential in the distal outflow tract, they have split into two discrete streams in the mid region of the control vessel (arrows in C). This is much less apparent in the *RockDN;Wnt1-cre* embryos (D). NCC have not penetrated the proximal outflow tract in either embryo. **E,F)** By E11.5 there are two discrete cushions (green and yellow) that spiral around one another in the control embryo; these appear fused along their length (the most proximal region is not in view) (E). In the *RockDN* mutant, the two cushions remain unfused and are still circumferential in the most distal region. The proximal tips of both cushions are pointing towards the right ventricle (arrows in F).

**Supplementary Methods**

**Mice and embryos**

Rock dominant-negative (*RockDN*) mice (1) (BRC no. 01294) from RIKEN BioResource Center (Tsukuba, Japan) were inter-crossed with the *ROSA 26R* reporter line (a gift from Prof. S. Bhattacharya, Oxford, UK (2)) or the *ROSAeYFP* reporter (JAX: 006148) line (3) and the *Wnt1-cre* line (a gift from Prof. S. Bhattacharya, Oxford, UK (4)). The *Tie2-cre* (JAX: 006148; (5)) line was intercrossed with the *ROSAeYFP* line. All mice were maintained on a C57Bl/6 background, backcrossed for 3 generations, then maintained by brother-sister matings. Mice were maintained according to the Animals (Scientific Procedures) Act 1986, United Kingdom, under project licence PPL 30/3876. All experiments were approved by the Newcastle University Ethical Review Panel.

*RockDN* female mice were heterozygous for the *RockDN* construct, whereas males were heterozygous for the *Wnt1-cre* construct, with resulting litters containing embryos of the genotypes, *RockDN*$^{+}$*;Wnt1-cre*$^{+}$ , *RockDN*$^{+}$*;Wnt1-cre*$^{-}$, *RockDN*$^{-}$*;Wnt1-cre*$^{+}$ *and RockDN*$^{-}$*;Wnt1-cre*$^{-}$; the latter three genotypes acted as controls. Litter mate controls were used in all experiments. The RockDN protein contains a point mutation in the Rho binding domain which prevents it from binding to RhoA. It binds to endogenous Rock1 and Rock2, and therefore inhibits the function of the endogenous kinase domain, thus interfering with function of both Rock isoforms and overcoming potential redundancy (1,6), whilst not affecting the function of other related kinases. Genotyping for *RockDN* and for the *CAT* box was performed as described (1). CD1 mice were obtained from Charles River.

**Quantitative real-time PCR**

Quantitative real time PCR was used to measure the relative quantities of the *CAT* gene cassette. Outflow tracts were dissected from four E11.5 control and four mutant

embryos and RNA was extracted using the Trizol reagent kit (Invitrogen). 1µg of RNA from each sample was treated with an initial DNase treatment step (Invitrogen DNase kit) and cDNA was produced by reverse transcription (Invitrogen SuperScript II RTase kit). Random 15-mers were used (Sigma).

The 7900ht fast real-time PCR system (Applied Biosystems) and the SYBR green JumpStart Taq ReadyMix kit (Sigma) were used for quantitative real-time PCR was All reactions were performed in triplicate. Two housekeeping genes were used for normalisation, *β-actin* and *GAPDH*, and were found to be stably expressed in this experimental setting. Relative quantities of gene expression were calculated using the ΔΔCt method. Primer sequences were for *β-actin*, F: 5'-GCTGGTCGTCGACAACGGCTC-3', R: 5'-CAAACATGATCTGGGTCATCTTTTC-3', for *GAPDH* F:5'-GCTGGTCGTCGACAACGGCTC-3', R:5'-CAAACATGATCTGGGTCATCTTTTC-3' and for *CAT* primers see (1).

**Chemical inhibition of Rock**

Pregnant CD1 females received daily injections of 1.5mg/kg body weight Y27632 or 5mg/kg body weight fasudil hydrochloride (Sigma), from embryonic days E9.5 to E12.5. The Rock inhibitors were dissolved in sterile 1x PBS. The embryos were collected at E14.5 and were dissected in cold PBS and fixed for two nights in 4% PFA and then processed for embedding into paraffin wax. 8µm sections were prepared and stained with αSMA (see Immunohistochemistry).

**β-galactosidase staining**

The embryos were dissected into ice-cold 1x PBS and the yolk sac or limb was retained for genotyping. The embryos were fixed in 4% PFA at 4°C. The length of time for fixation was dependent upon the age of the embryo. E8.5-E9.5, E10.5-E12.5 and E13.5-E15.5 embryos were fixed for five, 15 and 20 minutes respectively. The embryos were washed in 1x PBS and stained overnight at 37°C in staining solution

(wash buffer containing 1mg/ml X-gal in dimethyl formamide, 10mM K-ferricyanide, and 10mM K-ferrocyanide). The staining solution was removed and the embryos were washed in 1x PBS followed by fixation in 4% PFA for 24 hours (E8.5-E10.5) or 48 hours (E11.5-E15.5) as appropriate at 4°C. Embryos were then embedded in paraffin wax and sectioned. 1% aqueous eosin solution was used for counterstaining sections. For each stage of gestation, a minimum of three embryos were studied.

**Immunohistochemistry**

The embryos were dissected in ice-cold 1x PBS and fixed in 4% PFA at 4°C dependent upon the age of the embryo (overnight for E8.5-E11.5 and 48 hours for E12.5-E15.5). 8µm transverse of coronal tissue sections were cut and dried onto slides overnight at 37°C. The slides were placed in Histoclear (National Diagnostics) for dewaxing the sections, which were then hydrated through an ethanol gradient and treated with 3% $H_20_2$. The slides were washed in 1x PBS containing 0.1%Triton X and a 10% solution of fetal bovine serum (Sigma) was used for the blocking of sections.

The primary antibodies used for staining wax sections were GFP (Abcam) and α-smooth muscle actin (Sigma). Each antibody was diluted in 2% fetal bovine serum left overnight on the sections at 4°C. Following washing the sections in 1x PBS, the sections were then incubated at room temperature for one hour with either secondary anti-chicken IgY antibody conjugated to biotin (Abcam) or anti-mouse antibody conjugated to biotin (Dako) diluted in 2% fetal bovine serum. Avidin-biotin complex conjugated to horseradish peroxidase (Dako) treatment, and diaminobenzidine (Sigma) staining, was used to visualize immunoreactivity. The sections were counterstained in 0.5% aqueous methyl green solution and Histomount (National Diagnostics) was used for mounting slides. Images were captured using a Zeiss Axioplan microscope and Zeiss Axiovision software.

The embryos used for cryoembedding were washed through a series of sucrose solutions, 7.5% and 15%, then frozen in OCT embedding matrix (CellPath). 10µm sections were cut and fixed in 4% PFA. Following washing in 1x PBS, the sections were blocked 10% solution of fetal bovine serum (Sigma). Primary antibodies were diluted in 2% fetal bovine serum and incubated with the sections overnight at 4°C. The antibodies used in this study are GFP (Abcam), Rock1 (Abcam), Rock2 (Santa Cruz Biotechnology), β-catenin (BD Transduction Laboratories), connexin 43 (Chemicon) and caspase 3 (Abcam). Filamentous actin was stained with rhodamine-phalloidin (Sigma). Slides were then incubated at room temperature for one hour with secondary antibodies conjugated to Alexa fluorophores (Anti-chicken Alexa 488 fluor-conjugated and anti-rabbit Alexa 594 fluor-conjugated secondary antibodies, Life Technologies), diluted in 2% fetal bovine serum. Slides were mounted in Vectashield with DAPI (Vector Laboratories) and images were captured using a Zeiss Axioimager microscope with filters for DAPI, GFP, and Texas red and analysed using the Zeiss Axiovision software.

Experiments using either paraffin wax sections or frozen sections included a negative control in which primary antibody was absent; each experiment was repeated a minimum of three times.

**Haemotoxylin and eosin staining**

Staining was performed on PFA-fixed, paraffin embedded tissue sections. 8µm sections were cleared in Histoclear (National Diagnostics) then hydrated in an ethanol gradient, stained in haemotoxylin, de-stained in acid alcohol (1% HCl + 70% ethanol) and stained in 1% aqueous eosin. Sections were then dehydrated in an ethanol gradient, cleared in Histoclear and mounted in Histomount (National Diagnostics). Images were captured using a Zeiss Axioplan microscope and Zeiss Axiovision software.

**Elastin staining**

Slides were deparaffinised and rehydrated. After 5 minutes equilibration in PBS, slides were placed in Miller's elastin stain (Sigma) for 1 hour. They were carefully rinsed with $ddH_2O$ (10 dips) and then placed in 3% $FeCl_2$ for 10 minutes. The sections were the rinsed again in $ddH_2O$, as before, and counterstained with 1% aqueous eosin. After rinsing in $ddH_20$ to remove excess eosin, slides were dehydrated with 10 dips in butanol, placed in Histoclear for two 10 minute cycles and mounted with Histomount. Images were captured using a Zeiss Axioplan microscope and Zeiss Axiovision software.

**Neural crest cell cultures**

Neural folds from the hindbrain of E8.5-E9.5 embryos (control or *RockDN*$^+$*;Wnt1-cre*$^+$ embryos) were placed on coverslips coated in 0.5mg/ml poly-L-Lysine (Sigma) and 40μg/ml fibronectin (Sigma) (7). The explant was dissected and placed onto the coverslip and allowed to attach for 5 hours. They were then maintained in DMEM/10% FCS for 2 days, with 10μm Y27632 (Sigma) added on days 2-4. On day 5 the cells were washed in 1x PBS and fixed in 4% PFA and stained using the protocol for immunostaining of cryosections. The following antibodies were used on cells: rhodamine-phalloidin (Sigma), N-Cadherin (BD Transduction Laboratories) and connexin 43 (Chemicon).

**Three-dimensional reconstruction**

Serial sections were photographed from Xgal stained control and mutant embryos at E10.5 and E11.5 . The sections were aligned and three dimensional reconstructions were carried out using Amira 4.0 according to standard protocols (8).

**Cell quantification and statistical analysis**

NCC and EDC were counted in the arterial valve leaflets from a minimum of 3 sections from 3 separate embryos. Unstained cells were also counted so that the percentage of each lineage in the leaflets could be calculated. One-way ANOVA was used to test between numbers of NCC and endothelial-derived cells in the normal valve leaflets. T-test was used to compare numbers of NCC in the control and mutant valves, whereas a Chi squared test was used to search for an association between bicuspid valves and DORV.

**References**


1. Kobayashi K, Takahashi M, Matsushita N, Miyazaki J, Koike M, Yaginuma H, Osumi N, Kaibuchi K, Kobayashi K. Survival of developing motor neurons mediated by Rho GTPase signaling pathway through Rho-kinase. J Neurosci. 2004 Apr 7;24(14):3480-8.
2. Soriano P. Generalized lacZ expression with the ROSA26 Cre reporter strain. Nat Genet 1999 Jan;21(1):70-1.
3. Srinivas S, Watanabe T, Lin CS, William CM, Tanabe Y, Jessell TM, Costantini F. Cre reporter strains produced by targeted insertion of EYFP and ECFP into the ROSA26 locus. BMC Dev Biol. 2001;1:4.
4. Danielian PS, Muccino D, Rowitch DH, Michael SK, McMahon AP. Modification of gene activity in mouse embryos in utero by a tamoxifen-inducible form of Cre recombinase. Curr Biol. 1998 Dec 3;8(24):1323-6.
5. Kisanuki YY, Hammer RE, Miyazaki J, Williams SC, Richardson JA, Yanagisawa M. Tie2-Cre transgenic mice: a new model for endothelial cell-lineage analysis in vivo. Dev Biol. 2001 Feb 15;230(2):230-42.
6. Amano M, Chihara K, Nakamura N, Fukata Y, Yano T, Shibata M, Ikebe M, Kaibuchi K. Myosin II activation promotes neurite retraction during the action of Rho

and Rho-kinase. Genes Cells. 1998 Mar;3(3):177-188.

7. Moase CE, Trasler DG. Delayed neural crest cell emigration from Sp and Spd mouse neural tube explants. Teratology. 1990 Aug;42(2):171-82.
8. Soufan AT, Ruijter JM, van den Hoff MJB, de Boer PAJ, Hagoort J, Moorman AFM. Three-dimensional reconstruction of gene expression patterns during cardiac development. Physiol Genomics 2003; 13: 187–195 Aug;42(2):171-8.